

Correlation Effects on Atom Density Profiles of 1-D and 2-D Polarized Atomic-Fermi-Gas Loaded on Optical Lattice

M. Machida,^{1,2,*} S. Yamada,^{1,2,†} M. Okumura,^{1,2,‡} Y. Ohashi,^{3,2,§} and H. Matsumoto^{4,2,¶}

¹*CCSE, Japan Atomic Energy Agency, 6-9-3 Higashi-Ueno, Taito-ku Tokyo 110-0015, Japan*

²*CREST(JST), 4-1-8 Honcho, Kawaguchi, Saitama 332-0012, Japan*

³*Faculty of Science and Technology, Keio University, 3-14-1,*

Hiyoshi, Kohoku-ku, Yokohama, Kanagawa, 223-0061, Japan

⁴*IMR, Tohoku University, 2-1-1, Katahira, Aoba-ku, Sendai, Miyagi 980-8577, Japan*

(Dated: February 14, 2019)

We investigate effects of optical lattice potential in one- and two-dimensional two-component trapped Fermi gases with population imbalances. Using the exact diagonalization and the density matrix renormalization group methods complementarily, we calculate the atom density profile from the ground state many-body wavefunction as a function of attractive interaction strength for various population imbalances. The numerical results reveal that although a phase separation between the superfluid core and the shell cloud of excess atoms occurs as observed in experiments without the optical lattice, the population imbalance generally remains in the core region in contrast to the non-lattice cases. The essence of the numerical results in a strong attractive regime can be explained by an effective model composed of Cooper pairs and excess major fermions.

PACS numbers: 03.75.Ss, 71.10.Fd, 74.81.-g, 74.25.Jb

I. INTRODUCTION

Recently, two-component fermion systems with population imbalance have attracted much attention in various research fields, such as cold atoms, superconductors, and QCD [1]. In the 1960's, effects of the population imbalance have been theoretically investigated in the superconductivity literature [2, 3, 4]. Sarma considered the stability of an interior gap phase (Sarma state) [2]. Fulde and Ferrell [3], and Larkin and Ovchinnikov [4] predicted the so-called FFLO state, where the superconducting order parameter is spatially modulated. Very recently, some evidence of the FFLO state has been reported in a heavy fermion superconductor CeCoIn₅ [5].

The population imbalance has been also extensively studied in ultra-cold Fermi gases [6, 7, 8, 9, 10, 11]. The advantage of using atom gases is that one can widely tune some physical parameters, such as the interaction and the population imbalance. In a trapped two-component ⁶Li Fermi gas [6, 7, 8, 9, 10], a phase separation between a superfluid core region and a surrounding unpaired gas of excess atoms was observed. Recently, the absence of the population imbalance inside the superfluid core region was reported in [8, 10].

So far, the superfluid Fermi gas with population imbalance has been experimentally studied without an optical lattice [6, 7, 8, 9, 10, 11]. In this paper, we investigate effects of the lattice [12, 13, 14, 15] on the pop-

ulation imbalanced systems. Very recently, there have been several reports on this issue, one of which theoretically claims that FFLO is more stabilized than the non-optical lattice case [16], and others of which numerically show that FFLO is observable in the one-dimensional attractive Hubbard model [17] by using the density matrix renormalization Group (DMRG) method [18, 19]. Our approach in this paper differs from these works in using the exact diagonalization method mainly and the DMRG method [18, 19] complementarily in order to check whether the exact diagonalization results are small size effects or not. In addition, we focus on the density profile of majority (n_{\uparrow}) and minority components (n_{\downarrow}) at $T = 0$ in a one- and two-dimensional lattice trapped systems instead of the stability of the exotic superfluidity FFLO. The reason is that the atom density profile is the most convenient and clear observable for experiments. Moreover, the FFLO requires at least the population imbalance in the atom density profile. Namely, it is crucial point for FFLO whether the population imbalance survives even in the presence of pair instability at $T = 0$ ground state or not. Thus, we widely measure the atom density profiles in various system sizes, imbalance, interaction, dimensionality (1D-2D), and traps, prior to an examination of the FFLO stability. Consequently, we point out in a strongly-attractive interaction regime that correlation effects due to the presence of lattice result in a core phase with a typical population imbalance, which is very different from non-lattice cases [8, 10].

The contents of this paper are as follows. In Section II, we summarize the experimental results of the atom density profiles in the imbalanced Fermi gases without the optical lattice and show our prediction on those of the imbalanced gases in the presence of the optical lattice. Section III is devoted to explain the model and the numerical method. In Section IV, numerical results

*Electronic address: machida.masahiko@jaea.go.jp

†Electronic address: yamada.susumu@jaea.go.jp

‡Electronic address: okumura.masahiko@jaea.go.jp

§Electronic address: yohashi@rk.phys.keio.ac.jp

¶Electronic address: mhideki@mx1.ttcn.ne.jp

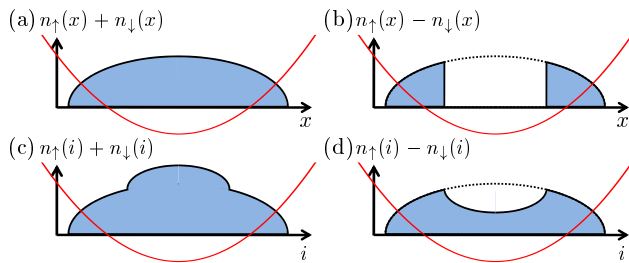


FIG. 1: Schematic profiles of the total atom density and the density difference between particles with pseudo-spin up and down, i.e., $n_{\uparrow} - n_{\downarrow}$, which are measured along the long axis of the trap for polarized fermionic gases. The upper panels (a) and (b) display the experimental (non-lattice system) results, while the lower panels (c) and (d) predict the profiles in the presence of the optical lattice. The parabolic lines schematically represent the trap potential shape. In the absence of the optical lattice, the experiments revealed that the phase separation between the paired (superfluid) gas and the completely polarized (excess major atoms only) periphery occurs as shown in the upper panels (a) and (b). On the other hand, the lower panels (c) and (d) show a typical result of numerical calculations in the presence of the optical lattice. A big difference between the upper and the lower panels is that the excess species can stay even on the superfluid core in the presence of the optical lattice.

by the exact diagonalization and DMRG are presented, theoretical analysis using an effective model derived in strong coupling limit is given, and strong trap effects are displayed as an exceptional case. Section V shows the results in two dimensional (2-D) systems, and Section VI discusses temperature effects on all the present results. Finally, summary and conclusion are given.

II. PARTICLE DENSITY PROFILES IN POLARIZED ATOMIC FERMI GASES

In this section, we summarize the experimental results [8, 10] of the trapped imbalanced Fermi gases without the optical lattice and predict how their results change by adding the optical lattice. Figure 1 (a) and (b) are schematic pictures of atomic density profiles obtained in experiments without the optical lattice, and (c) and (d) are our prediction of those in the presence of the optical lattice. At first, let us focus on Fig. 1 (a) and (b). The experiments revealed that the polarized gases show a phase separation between the core and the periphery below the superfluid transition temperature. The phase separation picture was clearly confirmed by monitoring the atom density profile for each of two Fermi-atom species. Inside the core, the profile shows an atom density ratio, $n_{\uparrow}(x) : n_{\downarrow}(x) = 1 : 1$ as shown in Fig. 1 (b) [8, 10], while a completely-polarized phase appears in the periphery, where the atom density ratio, $n_{\uparrow}(x) : n_{\downarrow}(x) = 1 : 0$ in a case that the majority species is Fermi atom with the pseudo-spin \uparrow .

On the other hand, our calculations in the presence of the optical lattice reveal that although the phase separation occurs like the experimental results without the optical lattice, the atom density profile shows a big difference compared to the non-lattice cases. We find in the presence of lattice that the population imbalance generally remains even in the superfluid core region, i.e., the atom density ratio inside the core, $n_{\uparrow}(i) : n_{\downarrow}(i) \neq 1 : 1$. Moreover, we find in sufficiently strong pairing-interaction that $n_{\uparrow}(i) : n_{\downarrow}(i) \simeq 2 : 1$ [20] inside the core as shown in Fig. 1 (d). This result is compared with an effective model theoretically derived in the strong limit of the attractive interaction. In this paper, we claim that correlation effects on the lattice bring about the imbalanced core phase. The main correlation effects on the lattice originate from a repulsive interaction between two Cooper pairs [21] and a site-exchange energy gain between a Cooper pair and an excess fermion as shown in IV. The effective model successfully explains why the imbalanced core emerges.

III. MODEL AND NUMERICAL CALCULATION METHOD

Let us show the model Hamiltonian and the numerical calculation method to obtain the ground state of the model. In this paper, we consider two-component trapped Fermi gases inside optical lattices with N lattice sites. When the optical lattice potential is sufficiently strong, the system can be well described by the Hubbard model, the one-dimensional (1-D) Hamiltonian of which is given as [22, 23],

$$H_{\text{Hubbard}} = -t \sum_{\langle i,j \rangle, \sigma} (a_{j\sigma}^{\dagger} a_{i\sigma} + \text{H.c.}) + U \sum_i n_{i\uparrow} n_{i\downarrow} + V \left(\frac{2}{N-1} \right)^2 \sum_{i,\sigma} n_{i\sigma} \left(i - \frac{N+1}{2} \right)^2, \quad (1)$$

where $a_{i\sigma}^{\dagger}$ is the creation operator of a Fermi particle with pseudo-spin $\sigma = \uparrow$ or \downarrow at i -th site, and U (< 0) is a pairing interaction. The summation $\langle i, j \rangle$ is taken over the nearest-neighbor sites, and the hopping matrix element t describes the hopping energy of atoms between the nearest-neighbor sites. The last term in Eq. (1) gives a harmonic trap potential, in which V corresponds to the potential height at the edge of the lattice. At the edge, the open-boundary condition is imposed. If the atomic density profile drops down at the edge, then the boundary condition does not almost affect the result. The parameter V and the total number of Fermi atoms N_{F} are selected to sufficiently reduce the atom density at the edges.

In this paper, we examine various population imbalances with keeping $N_{\uparrow} \geq N_{\downarrow}$ ($N_{\text{F}} = N_{\uparrow} + N_{\downarrow}$), where N_{\uparrow} and N_{\downarrow} are the total number of Fermi atoms with pseudo-spin \uparrow and \downarrow , respectively. In 1-D cases, we numerically

diagonalize the Hamiltonian, Eq. (1) to calculate the density profile at $T = 0$. Although this approach gives us exact results, the accessible system size is severely limited. To compensate this disadvantage and confirm whether the exact diagonalization results are small size effects or not, we employ the DMRG method. The DMRG guarantees a high accurate result as long as the trap potential is not so steep. We confirm that a difference between the eigen-values obtained by both methods is below 10^{-6} in the lattice size $N = 20$ with $V/t = 1$. Since the DMRG is mainly used for much less steep traps (V/t is fixed to be 1 except for Section VI D, which examines a trap strength dependence), the DMRG results sufficiently keep high accuracy.

On the other hand, in two-dimensional (2-D) square lattice systems, we use the exact diagonalization solely, because the method is now the most accurate and reliable for 2-D finite systems. Here, we just mention that the direct extension of the DMRG to 2-D ladder cases, which keeps high accuracy like 1-D cases is now under development [24, 25]. For the exact diagonalization and the DMRG, we use SX-6 (1-node 4 CPU's system) and Altix 3700Bx2 (scalar parallel machine) in JAEA and the Earth Simulator [26]. In the exact diagonalization, the problems with the lattice size $N = 16$ are calculated by SX-6, while those with above $N = 20$ the Earth Simulator. In the latter case, we need parallelization and high-performance computing techniques. See Ref. [26] for computational technical issues on massively parallel supercomputers. On the other hand, all DMRG calculations are made on Altix 3700Bx2.

IV. NUMERICAL RESULTS FOR 1-D IMBALANCED GASES

A. Exact Diagonalization Studies

Let us present exact diagonalization results for the imbalanced 1-D attractive Hubbard model with the trap potential. Figure 2 shows U/t dependences of the calculated atom-density profile of the ground state, $n(i) = n_{\uparrow}(i) + n_{\downarrow}(i)$ for three population imbalances, whose ratios of major to minor species are (a) 5:3, (b) 6:2, and (c) 7:1, respectively. For these three cases, the lattice size $N = 16$, the total number of fermions $N_F = 8$, and $V/t = 1$. The filling is just the quarter one if the trap potential is absent. Although the depression at the edges is not completely zero in the presence of the trap ($V/t = 1$), we confirm that there are no edge effects because of no significant change of profiles on the lattice size extension (to $N = 18$ and 20) with the same fermion number (see Fig. 2 (d)).

In each panel, we find a step-like structure (see arrow in each figure) in each dome like profile. This structure becomes more pronounced as one increases the amplitude strength of the attractive interaction $|U|$. The structure is also observable in Fig.2(d) with a larger size ($N = 20$),

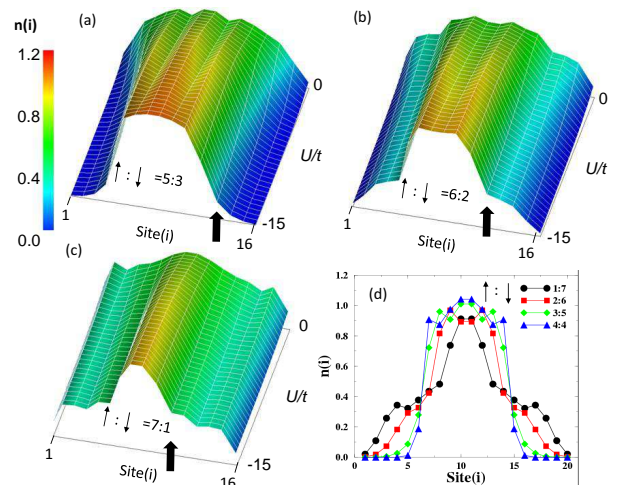


FIG. 2: The exact diagonalization results for U/t dependences ($-15 \leq U/t \leq 0$) of particle density profiles, $n(i)$ for three imbalance cases, whose ratios of major to minor fermion species are (a) 5:3, (b) 6:2, and (c) 7:1, respectively. In these three cases, $N_F = 8$, $N = 16$ and $V/t = 1$. The panel (d) is a highlight of $n(i)$ at $U/t = -10$ for the imbalance from 4:4 to 7:1 in $N = 20$. N_F and V/t are the same as (a-c).

in which N_F and V/t is the same as (a-c), and U/t is fixed to be -10 .

The step-like structures seen in Fig. 2 are found to be associated with the phase separation between a core phase whose main component is pair and a shell one composed of only un-paired excess atoms from other observables as shown in Fig. 3. Figure 3 (a), (b), (c) and (d), respectively, show U/t dependent profiles of the single-occupation density $n_F(i)$, the double-occupation density $n_B(i)$, the density subtraction $n_{\uparrow}(i) - n_{\downarrow}(i)$, and the on-site pair amplitude $\Delta(i)$ [23, 27] defined by

$$\Delta(i) = \frac{1}{\sqrt{2}} \langle N_{\uparrow} + 1, N_{\downarrow} + 1 | a_{i\uparrow}^{\dagger} a_{i\downarrow}^{\dagger} | N_{\uparrow}, N_{\downarrow} \rangle \quad (2)$$

where, $|N_{\uparrow}, N_{\downarrow}\rangle$ is the ground state wavefunction with $(N_{\uparrow}, N_{\downarrow})$ atoms. This function is a probe for the local condensate amplitude [27] for finite systems. Here, we note that the probe gives non-zero values even at the interaction free ($U/t = 0$) as seen in 3 (d) and shows spatial modulations without sign changes especially in a relatively-weak interaction regime. The reason for the former one is that the function counts all the possible pair formation probabilities on a local site, i.e., it includes even the pair formation due to the trap potential, and that for the latter one may be that the strong confinement effect masks the sign change due to the FFLO. Although this latter interpretation requires further examinations, we confirm at least the growth of the local condensate amplitude. See Ref.[17] for the spatial pair correlation in larger core phases. $n_F(i)$ and $n_B(i)$ are calculated by picking up the coefficient of the eigen-state whose i -th site occupation is 1 and 2, respectively, from the ground state wave-function and summing up the am-

plitude of the coefficients. Their explicit operator definitions are given by $n_F(i) = \langle n_\uparrow(i) + n_\downarrow(i) \rangle - n_B(i)$, where $n_B(i) = \langle n_\uparrow(i)n_\downarrow(i) \rangle$. For the methodological details to calculate $n_F(i)$ and $n_B(i)$, see Ref. [21]. According to Ref. [21], as $|U/t|$ increases in the balanced case, $n_F(i)$ decreases, while $n_B(i)$ instead increases. This simple relationship means that the Cooper pair becomes more tightly-bounded one on a site with increasing $|U/t|$.

From Fig. 3, we clearly find that $n_B(i)$ and $\Delta(i)$ will develop only inside the “phase boundary” characterized by the step-like structure as seen in Fig. 2 while they completely diminish outside the boundary (shell region) [28]. This tendency becomes more pronounced with increasing the attractive interaction and somewhat saturated in the strong limit. This suggests that the pair density and the superfluid order (phase rigidity) locally develop inside the core. This does not contradict a consensus that the superfluid correlation grows as the most dominant one in 1-D attractive Hubbard model [29] although any correlations algebraically decay in 1-D systems. Thus, we call the core region “superfluid core” in the following. However, we note that there is a subtle issue whether the whole core really exhibits superfluidity in non-zero temperature due to its dimensionality and finiteness or not. The discussion originates from a problem whether the phase rigidity grows and survives from an edge of core to another edge against fluctuations. This is beyond information obtained by the present analysis of the exact diagonalization and DMRG. Thus, we do not discuss the stability of the superfluidity but concentrate only on atom density profiles in the ground state in this paper. We believe that the future experiments and more advanced theoretical and numerical methods resolve the problem (e.g., see Ref. [17] for the static non-local correlation of the pair function inside the core phase).

Let us turn back to atom density profile in the presence of lattice, again. Fig. 3 (a) reveals that un-paired component stays even in the core region, where the $n_B(i)$ and $\Delta(i)$ grow. As a result, the density difference $\delta n(i) \equiv n_\uparrow(i) - n_\downarrow(i)$ does not vanish in the core region as seen in Fig. 3 (c). Generally, we find that $n_\uparrow(i) : n_\downarrow(i) \simeq 2 : 1$ in the core region except for a very weak coupling regime (compare Fig. 2(b) with Fig. 3(c)). This feature is clearly seen in Fig.4(a-c), which display slices of $n_\uparrow(i)$ and $n_\downarrow(i)$ profiles for $U/t = -15, -5$, and -1 , respectively. Inside this range, it is found that the ratio is approximately $2 : 1$. Also, the ratio is seen for other imbalance cases (see e.g., Fig. 4 (d)), although there is a small deviation from $2 : 1$. This is quite different from the experimental result in the absence of the lattice, where one obtains $n_\uparrow(i) : n_\downarrow(i) \simeq 1 : 1$, or $\delta n(i) \simeq 0$ in the core region [8, 10].

B. DMRG Studies

In order to confirm the generality of the phase separation and the core phase characterized by the approx-

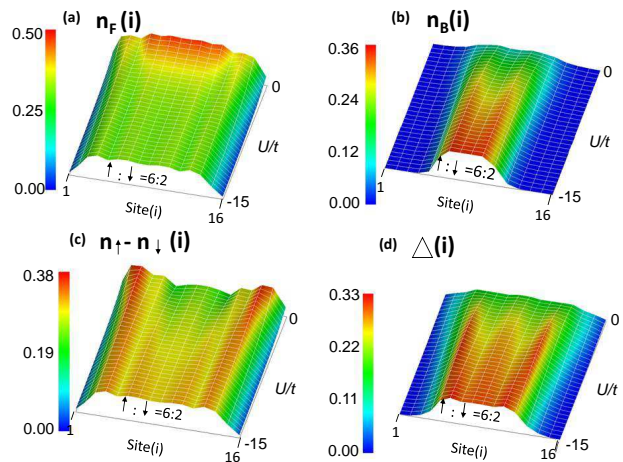


FIG. 3: The exact diagonalization results for U/t dependences ($-15 \leq U/t \leq 0$) of profiles of (a) the single occupation density $n_F(i)$, (b) the double occupation density $n_B(i)$, (c) the subtraction from major to minor species density $n_\uparrow(i) - n_\downarrow(i)$, and (d) the on-site pair amplitude $\Delta(i)$. In all the cases, $N_F = 8$ ($6 \uparrow, 2 \downarrow$), and other conditions are the same as those of Fig. 1 (a-c).

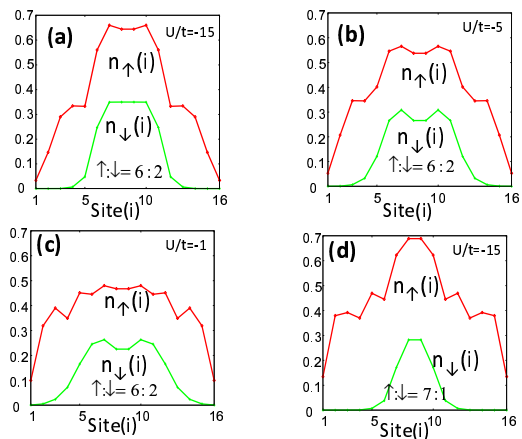


FIG. 4: The exact diagonalization results of $n_\uparrow(i)$ and $n_\downarrow(i)$ profiles for (a) $U/t = -15$, (b) -5 , and (c) -1 . The numerical condition is the same as the case of Fig.2(b), in which the imbalance ratio is $3 : 1$. (d) $n_\uparrow(i)$ and $n_\downarrow(i)$ profiles for $U/t = -15$ in the case of the imbalance ratio $7 : 1$.

imate ratio “ $2 : 1$,” we adopt the DMRG method and study much larger systems ($N = 80$ and 160). Figure 5 (a) and (b) show U/t dependences ($-15 \leq U/t \leq 0$) of density profiles for major and minor species, respectively, and Fig. 5 (c) is their subtraction. In their results, the lattice size $N = 80$, $N_F = 32$, and the prepared ratio of different atom species is $3 : 1$. It is found from Fig. 5 (a-b) that the atomic density ratio in the core region is about “ $2 : 1$ ” except for the weak coupling region. The Fig. 5 (d) and (e) are two slices ($U/t = -15$ and -5) of profiles of n_\uparrow and n_\downarrow , which clearly exhibit the approximate ratio “ $2 : 1$ ”. In addition, Fig. 5 (f), which shows

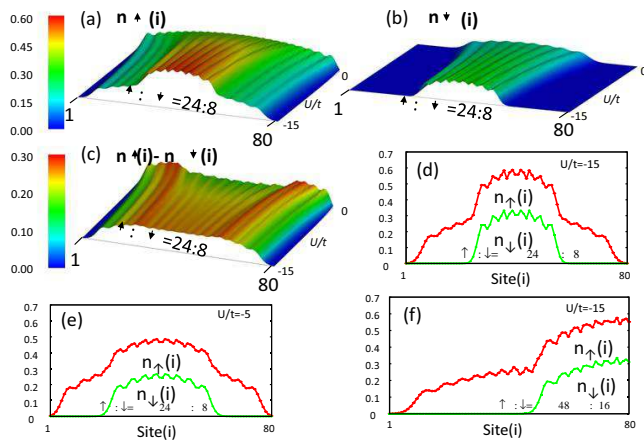


FIG. 5: The DMRG results of U/t dependences ($-15 \leq U/t \leq 0$) for density profiles for (a) major species $n_{\uparrow}(i)$, (b) minor ones $n_{\downarrow}(i)$, and (c) the subtraction from major to minor one $n_{\uparrow}(i) - n_{\downarrow}(i)$. In these panels, $N = 80$, and $N_F = 32$ ($24 \uparrow, 8 \downarrow$). The panel (d) and (e) are two slices for $U/t = -15$ and -5 for $n_{\uparrow}(i)$ and $n_{\downarrow}(i)$, and the panel (f) is a half left-side profile of the local density of $n_{\uparrow}(i)$ and $n_{\downarrow}(i)$ for $N = 160$, $N_F = 62$ ($\uparrow 48, \downarrow 16$), and $U/t = -10$. In all cases, $V/t = 1$.

DMRG result (a half profile) of n_{\uparrow} and n_{\downarrow} for $N = 160$ and $N_F = 64$, is also a clear demonstration of the approximate “2 : 1.” In these cases, it is noted that the trap potential and the resulting confinement is relatively very weak compared to the exact diagonalization results. From the common results by both numerical methods, the approximate ratio $n_{\uparrow} : n_{\downarrow} \simeq 2 : 1$ is widely expected to be observed in the strong coupling regime in the presence of the optical lattice with harmonic traps.

C. Effective Model and Discussion

Both the exact diagonalization and the DMRG reveal that the excess un-paired atoms remain even inside the core region in contrast to the experimental results without the optical lattice. Especially, the ratio of majority to minority species is approximately “2:1” inside the core in the strong coupling regime. This result is considered to clearly originate from strong correlation effects due to the presence of lattice. Here, we derive an effective model in order to explain the findings. In the strong-coupling limit $|U| \rightarrow \infty$, one finds that the present lattice Fermi gas is effectively described by a gas mixture of unpaired free Fermi-atoms and dimer atoms [21, 30]. The effective Hamiltonian has the form, (dropping the potential term)

$$\begin{aligned}
 H_{\text{Hubbard}} \rightarrow & 2t^2/U \sum_i (n_{i+1}n_i - B_{i+1}^{\dagger}B_i) \\
 & - t \sum_i (a_{i+1,\uparrow}^{\dagger}a_{i,\uparrow} + \text{H.c.}) \\
 & t \sum_i (a_{i+1,\uparrow}^{\dagger}B_{i+1}B_i^{\dagger}a_{i,\uparrow} + \text{H.C.}). \quad (3)
 \end{aligned}$$

Here, B_i^{\dagger} is a creation operator of a bound pair at the i -th site. In this effective Hamiltonian, the first term gives the nearest-neighbor repulsive interaction $U_{\text{eff}} \equiv 2t^2/U$ between Cooper-pair bosons and the energy gain of the molecular hopping $-t_{\text{eff}} \equiv -2t^2/U$ between the nearest-neighbor sites. The second term in Eq. (3) stands for the kinetic energy of excess \uparrow -spin atoms, and the third term describes an exchange energy between a Cooper pair and an excess atom when they sit on the nearest neighbor position each other. The third term is also derived by considering the hopping of the minor atom from an on-site Cooper pair to the nearest neighbor site, in which an excess major atom solely stays. This effective model is valid in $|U| \rightarrow \infty$, since there exists conversion process between the bosons and the excess fermions for finite negative U/t . However, it is numerically found that the limit description ($|U| \rightarrow \infty$) becomes sufficiently good more than $|U/t| \sim 10$, since the un-paired fermions almost disappear in the range. See Ref. [21] for U/t dependence of the total number of un-paired fermions ($\equiv \sum_i n_F(i)$) in the balanced cases.

In the effective model considering only the first term of Eq. (3), i.e., in the balanced cases, it is well-known that the pair density correlation function shows a large magnitude between every other sites. The reason is that the Cooper pair tends to occupy every other site to avoid energy loss by the nearest-neighbor repulsion between Cooper-pair bosons (see the first term of Eq. (3)). As a result, such a correlation effect causes a static spatial modulation of the pair density in the presence of the trap, which breaks the translational symmetry. In other words, a degeneracy between two dominant states having the site density correlation of pairs as “ $-n_{\uparrow\downarrow} - 0 - n_{\uparrow\downarrow} - 0$ ” and “ $-0 - n_{\uparrow\downarrow} - 0 - n_{\uparrow\downarrow}$ ”, where $n_{\uparrow\downarrow}$ is the site density of the Cooper pair ($n_{\uparrow\downarrow} < 1$), is broken by the trap potential, and the static density modulation as represented by “ $-n'_{\uparrow\downarrow} - n''_{\uparrow\downarrow} - n'_{\uparrow\downarrow} - n''_{\uparrow\downarrow}$ ” appears. This behavior in the balanced case was also confirmed by different authors [21, 31, 32].

On the other hand, in the imbalanced systems, both the first and third terms of Eq. (3) explain the present numerical results of the density profiles. The first term prefers two degenerate density correlations described above, and excess atoms can then find their positions in the nearest neighbor sites of the on-site pair. Furthermore, the third term stabilizes the two density-correlation profiles, in which excess majority atoms slip in like “ $-n_{\uparrow\downarrow} - n_{\uparrow} - n_{\uparrow\downarrow} - n_{\uparrow}$ ” and “ $-n_{\uparrow} - n_{\uparrow\downarrow} - n_{\uparrow} - n_{\uparrow\downarrow}$ ”, since the energy $2t$ is gained by an anti-bonding exchange between an on-site pair and its neighbor excess atom. As a result, one finds that the density difference in the core region is simply given by $n_{\uparrow} : n_{\downarrow} \simeq 2 : 1$ in the large $|U|$ range. We emphasize that the presence of the lattice is responsible for the approximate ratio 2 : 1 while it is absent in a Fermi gas with no lattice potential.

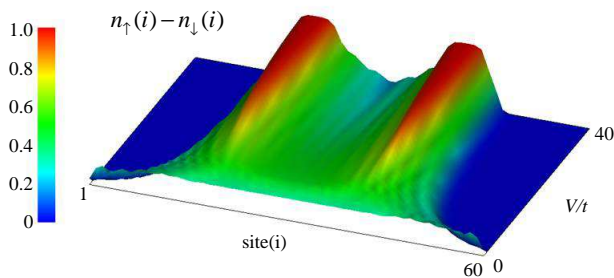


FIG. 6: The DMRG results of V/t dependence of the particle density profile for $N = 60$, $N_F = 40$ ($30 \uparrow, 10 \downarrow$), and $U/t = -10$.

D. Strong Trap Effect

In this subsection, we study a confinement force dependence on the atom density profile. Figure 6 shows V/t dependence on the density profile for the imbalance ratio $N_\uparrow : N_\downarrow = 3 : 1$. The focus of interest is a case in which the strength of the trap potential is so strong that the confinement force overwhelms the correlation effects due to the presence of lattice, i.e., the repulsive interaction between Cooper pairs and the exchange energy gain between a Cooper pair and an excess atom as explained above. Such an extreme situation is observable above $V/t \sim 35$ as seen in Fig. 6. One finds above $V/t \sim 35$ that un-paired atoms are excluded from a central part of the core region. Then, the density difference from major to minor species becomes $\delta n(i) \simeq 0$, namely, the ratio $n_\uparrow : n_\downarrow \simeq 1 : 1$. This feature is equivalent with the recent experiments without lattices [8, 10]. However, such a situation may be non-realistic, since it requires very large V compared to the non-lattice one. Moreover, the numerical simulation result (Fig. 6) reveals that only a central point of the core region shows $n_\uparrow : n_\downarrow = 1 : 1$. This is also not experimentally observable in non-lattice cases. It is found even in strongly confined cases that the lattice presence is non-negligible.

V. NUMERICAL RESULTS FOR 2-D IMBALANCED GASES

In this section, we study 2-D imbalanced gases in the presence of the optical lattice. The lattice is a square one, in which only the nearest neighbor hopping is allowed. In this paper, we employ only the exact diagonalization. Thus, the total number of lattice sites N is limited to 25, and $N_F = 12$, where the imbalance ratio $n_\uparrow : n_\downarrow = 3 : 1$ ($9 \uparrow, 3 \downarrow$).

Figure 7 shows a typical result of the calculated density profiles for $n_\uparrow(i)$, $n_\downarrow(i)$, and their subtraction $n_\uparrow(i) - n_\downarrow(i)$ in a two-dimensional lattice Fermi gas, in which 5×5 ($= 25$) square lattice is used, and U/t and V/t are taken -15 and 1 , respectively. Although the system size is small, we find $n_\uparrow : n_\downarrow \simeq 2 : 1$ inside the core, again.

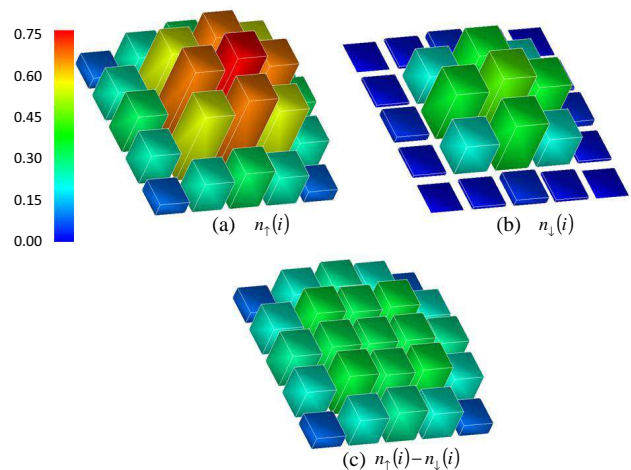


FIG. 7: The exact diagonalization results of the particle density profiles of (a) $n_\uparrow(i)$, (b) $n_\downarrow(i)$ and (c) $n_\uparrow(i) - n_\downarrow(i)$ for 2-D attractive imbalanced Hubbard model with a 2-D harmonic trap potential. In this case, $N = 25$, $N_F = 12$ ($9 \uparrow, 3 \downarrow$), $U/t = -15$, and $V/t = 1$.

This result indicates that the penetration of un-paired excess atoms into the core region is a general feature in the presence of a lattice, irrespective of dimensionality of the system.

VI. FINITE TEMPERATURE EFFECTS

Finally, let us mention finite temperature effects on the approximate ratio 2:1 in the core phase. We find that there are two crucial temperatures in discussing the temperature effects on the present results. The first temperature, which is much higher than the second temperature, is given by an energy scale in which the Hubbard model becomes sufficiently valid, i.e., the single-band Hubbard model is a good description. The experiments have already succeeded in reaching a range below the first temperature. The second temperature is characterized by a lower energy range that the correlation effects have an important role, i.e., the present features become effective. Thus, the problem is whether one can cool down below the second temperature or not. Let us estimate the second temperature. In the half-filling of 1-D lattice, $0.5t \sim E_F$, where E_F is the Fermi energy and t is the hopping matrix element in the Hubbard model, while the energy scale for the main correlation effect is t^2/U as shown in Eq. (3) in this manuscript. Thus, if one assumes $U/t \sim 10$, then the energy scale for the correlation $\sim 0.1t$. This means that the correlation effect becomes effective when the temperature is lower than $0.2E_F$. The temperature range $T < 0.2E_F$ was achieved in the absence of the optical lattice.

VII. SUMMARY

We investigated ground state properties of two-component trapped Fermi gases with population imbalances loaded on optical lattices. Using the exact diagonalization method and partly DMRG, we calculated the density profiles for 1-D and 2-D Hubbard model, as a function of the attractive interaction for various population imbalances. We showed that the population imbalance remains in the core phase, where the ratio of major to minor species, $n_{\uparrow} : n_{\downarrow} \simeq 2 : 1$. This result is observed in the wide parameter range except for the weak attractive interaction or the extremely strong trap one irrespective of the dimensionality. This is different from the case in the absence of the lattice, where $n_{\uparrow} : n_{\downarrow} = 1 : 1$ is observable in the core region. The character in the core phase on the optical lattice can be explained by the correlation effects on the lattice through the effective model.

Note added — Recently, we became aware of Refs. [16, 17], which analyze the same model and give consistent results with ours.

Acknowledgments

M.M. would like to thank T. Koyama, M. Kato, T. Ishida, H. Ebisawa, and N. Hayashi for helpful discussions about superconductivity. He also thanks Y. Morita for his support, and T. Imamura, T. Kano and staff members in the Earth Simulator center for their supports in large-scale calculations. Two of authors (M.M. and S.Y.) acknowledge M. Kohno, T. Hotta, and H. Ohnishi for illuminating discussion about the DMRG techniques. The work was partially supported by Grant-in-Aid for Scientific Research on Priority Area “Physics of new quantum phases in superclean materials” (Grant No. 18043022 and 18043005) from the Ministry of Education, Culture, Sports, Science and Technology of Japan. In addition, this work was supported by Grant-in-Aid for Scientific Research from MEXT, Japan (Grant No. 16740187, 17540368, 18500033, 18540387, and 17540368), and performed under a support by JSPS Core-to-Core Program-Strategic Research Networks “Nanoscience and Engineering in Superconductivity (NES)”.

-
- [1] See, e.g., R. Casalbuoni and G. Nardulli, *Rev. Mod. Phys.* **76**, 263 (2004); D. E. Sheehy and L. Radzihovsky, *Ann. Phys.* **322**, 1790 (2007); K. Levin and Q. Chen, *cond-mat/0610006*.
- [2] G. Sarma, *J. Phys. Chem. Solids* **24**, 1029 (1963).
- [3] P. Fulde and R. A. Ferrell, *Phys. Rev.* **135** A550 (1964).
- [4] A.I. Larkin and Y.N. Ovchinnikov, *Zh. Eksp. Teor. Fiz.* **47**, 1136 (1964) [*Sov. Phys. JETP*, **20**, 762 (1965)].
- [5] See, e.g., K. Kumagai, M. Saitoh, T. Oyaizu, Y. Furukawa, S. Takashima, M. Nohara, H. Takagi, and Y. Matsuda, *Phys. Rev. Lett.* **97**, 227002 (2006); K. Kakuyanagi, M. Saitoh, K. Kumagai, S. Takashima, M. Nohara, H. Takagi, and Y. Matsuda, *ibid* **94**, 047602 (2005).
- [6] M. W. Zwierlein, A. Schirotzek, C. H. Schunck, and W. Ketterle, *Science* **311**, 492 (2006).
- [7] M. W. Zwierlein, A. Schirotzek, C. H. Schunck, and W. Ketterle, *Nature* **442**, 54 (2006).
- [8] Y. Shin, M. W. Zwierlein, C. H. Schunck, A. Schirotzek, and W. Ketterle, *Phys. Rev. Lett.* **97**, 030401 (2006).
- [9] G. B. Partridge, W. Li, R. I. Kamar, Y. A. Liao, and R. G. Hulet, *Science***311**, 503 (2006).
- [10] G. B. Partridge, W. Li, R. G. Hulet, M. Haque, and H. T. C. Stoof, *Phys. Rev. Lett.* **97**, 190407 (2006).
- [11] C. H. Schunck, Y. Shin, A. Schirotzek, M. W. Zwierlein, and W. Ketterle, *Science* **316**, 867 (2007).
- [12] M. Greiner, O. Mandel, T. Esslinger, T. Hänsch, and I. Bloch, *Nature* **415**, 39 (2002).
- [13] M. Köhl, H. Moritz, T. Stöferle, K. Günter, and T. Esslinger, *Phys. Rev. Lett.* **94**, 080403 (2005).
- [14] J. K. Chin, D. E. Miller, Y. Liu, C. Stan, W. Setiawan, C. Sanner, K. Xu, W. Ketterle, *Nature* **443**, 961-964 (2006).
- [15] For recent reviews, see, e.g., I. Bloch, *Nature Physics* **1**, 23 (2005); D. Jaksch and P. Zoller, *Ann. Phys.* **315**, 52 (2005); M. Lewenstein, A. Sanpera, V. Ahufinger, B. Damski, A. Sen(De), and U. Sen, *Adv. Phys.* **56**, 243 (2007), and references therein.
- [16] T. K. Koponen, T. Paananen, J.-P. Martikainen, and P. Törmä *Phys. Rev. Lett.* **99**, 120403 (2007).
- [17] A. E. Feiguin and F. Heidrich-Meisner, *Phys. Rev. B* **76**, 220508(R) (2008); M. Tezuka, and M. Ueda, *Phys. Rev. Lett.* **100**, 110403 (2008); A. Lüscher, R. M. Noack, and A. M. Läuchli, *arXiv:0712.1808*; M. Rizzi, M. Polini, M. A. Cazalilla, M. R. Bakhtiari, M. P. Tosi, and R. Fazio, *arXiv:0712.3364*.
- [18] S. R. White, *Phys. Rev. Lett.* **69**, 2863 (1992); *Phys. Rev. B* **48**, 10345 (1993).
- [19] For recent reviews, see, e.g., U. Schollwöck *Rev. Mod. Phys.* **77**, 259 (2005); K. Hallberg, *Adv. Phys.* **55**, 477 (2006), and references therein.
- [20] Here, we note that $n_{\uparrow} : n_{\downarrow} = 2 : 1$ does not mean the double and the single occupations of a site by atoms, respectively. An atom is generally delocalized over several sites. Therefore, $n_{\sigma}(i)$ can become less than 1 if the filling is below the half-filling without the trap potential. The ratio 2:1 in the core region as shown in Fig. 1 (b) indicates the ratio of the observable atomic densities on a single site.
- [21] M. Machida, S. Yamada, Y. Ohashi, and H. Matsumoto, *Phys. Rev. A* **74**, 053621 (2006).
- [22] M. Rigol, A. Muramatsu, G. G. Batrouni, and R. T. Scalettar, *Phys. Rev. Lett.* **91**, 130403 (2003).
- [23] M. Machida, S. Yamada, Y. Ohashi, and H. Matsumoto, *Phys. Rev. Lett.* **93**, 200402 (2004).
- [24] S. Yamada, M. Okumura, and M. Machida, *arXiv:0707.0159*.
- [25] M. Machida, M. Okumura, and S. Yamada, *Phys. Rev. A* **77**, 033619 (2008).
- [26] S. Yamada, T. Imamura, T. Kano, and M. Machida, *Proc. of SC2006*; <http://sc06.supercomputing.org/schedule/pdf/gb113.pdf>.

- [27] Eq. (2) gives the pair condensate amplitude in finite systems. When the amplitude develops, it indicates that the ground state is dominated by the condensed pairs. See, e.g., L. P. Gor'kov, *Sov. Phys. JETP* **34**, 505 (1958); J. Bardeen, *Phys. Rev. Lett.* **9**, 147 (1962); P. G. de Gennes, *Superconductivity of metals and alloys*, Advanced Book Classic (Westview Press, Boulder, 1999) p109, Eq. (4.57).
- [28] Here, it should be noted that the reason why the distribution of $\Delta(i)$ deviates from that of $n_B(i)$ is a finite size effect (see the definition, Eq. (2)).
- [29] V. J. Emery, in *Highly Conducting One-Dimensional Solids*, ed. b J. T. Devreese, R. P. Evrard, and V. E. van Doren (Plenum, New York, 1978), p.247; H. Fukuyama and H. Takayama, in *Electronic Properties of Inorganic Quasi-One Dimensional Compounds*, ed. by P. Monceau (Reidel, Dordrecht, 1985), p.41.
- [30] L. Belkhir and M. Randeria, *Phys. Rev. B* **45**, 5087 (1992).
- [31] Gao Xianlong, M. Rizzi, M. Polini, R. Fazio,2, M. P. Tosi, V. L. Campo, Jr., and K. Capelle, *Phys. Rev. Lett.* **98**, 030404 (2007).
- [32] R. A. Molina, J. Dukelsky, and P. Schmitteckert, *Phys. Rev. Lett.* **99**, 080404 (2007).